International Journal of Biological Macromolecules 148 (2020) 276–283

Contents lists available at ScienceDirect

International Journal of Biological Macromolecules

journal homepage: http://www.elsevier.com/locate/ijbiomac

Design and fabrication of a label-free aptasensor for rapid and sensitive detection of endoglucanase

Fataneh Fatemi

Protein Research Center, Shahid Beheshti University G.C., Tehran, Iran

ARTICLE INFO

Article history:
Received 29 September 2019
Received in revised form 11 December 2019
Accepted 4 January 2020
Available online 7 January 2020

Keywords:
Endoglucanase II
RGO/AuNPs nanoparticles/EGII DNA aptamer
Electrochemical aptasensor

ABSTRACT

Endoglucanase (endocellulase, EC 3.2.1.4) is one of the most widely used enzymes in industry. Despite its importance, improved methods for the rapid, selective, quantitative assay of this enzyme have been slow to emerge. In this work, we have designed an aptasensor platform for ultrasensitive endoglucanase II detection based on DNA aptamer and reduced graphene oxide/Au nanoparticles (RGO/AuNPs). The surface morphology of RGO/AuNPs was characterized by various techniques such as transmission electron microscopy (TEM), X-ray diffraction (XRD), energy-dispersive X-ray spectroscopy (EDX) methods. The aptasensor characterization was monitored with electrochemical techniques. Using RGO/AuNPs as a nanomaterial can effectively increase the conductivity of biosensor electrode. Moreover, using an RGO/AuNPs/aptamer platform in the presence of endoglucanase, the sensor system is able to generate a signal, which significantly improves the selectivity of the aptasensor. The fabricated aptasensor exhibits high sensitivity and selectivity to endoglucanase II with a low limit of detection (LOD) ˜0.1 nM.

1. Introduction

Cellulose is the most-abundant and low-cost renewable natural organic compound. It contains a glucose polymer linked by a β-1,4-glycosidic bond and can be hydrolyzed by the cellulase enzyme. Cellulase is a hydrolytic enzyme that has been widely used in renewable energy sources for cellulosic ethanol production and biomass conversion. It also has a multitude of biofriendly applications across the pharmaceutical, textile, detergent, and food industries [1]. According to a market report published by Transparency Market Research, the cellulase segment is projected to grow at the highest rate between 2017 and 2022 and has become the fastest growing industrial enzyme globally [2].

Generally, cellulase is characterized by noncomplex or multicomponent enzyme complexes, operating synergistically. In different species like *Aspergillus niger*, cellulase is represented mainly by noncomplex systems (e.g., endoglucanase), which is most advantageous for industrial application [3]. Cellulase hydrolyzes the cellulose polymer chain by hydrolytic cleavage of the β-1,4-glycosidic bond in several steps. Depending on the site of cleavage, it is classified as endo1,4-glucanase (endoglucanase, E.C 3.2.1.4), ß-glucosidase (E.C 3.2.1.21), or exoglucanase (E.C 3.2.1.91). Endoglucanase is the major cellulolytic component enzyme and has the highest catalytic activity among other constituents of the cellulase enzymatic complex [4]. Endoglucanases randomly cleave the intramolecular β-1,4-glycosidic bonds in the amorphous cellulose region and produce the oligosaccharides [5]. It is generally believed that the market for endoglucanases enzymes will increase dramatically when the second-generation biofuel industry becomes economical.

In the cellulose industry applications and bioproduction of cellulase enzymes by microorganisms, the complexity arises from finding the particular method that can be used to detect each cellulolytic enzyme and quantifying produced cellulase activity. In biological materials and microbial fermentation broths, endoglucanase detection can be measured by the decrease in viscosity of water-soluble, chemically modified cellulose derivatives such as carboxymethyl cellulose 7 M and rates of hydrolysis of colorimetric or non-colorimetric substrates such as nitrophenyl-cello-oligosaccharides, cello-oligosaccharides, borohydride reduced cello-oligosaccharides, and benzylidene end-blocked 2-chloro-4-nitrophenyl-β-cellotrioside [6–8]. However, these substrates cannot be used to measure endoglucanase in the presence of other cellulose-degrading enzymes such as β-glucosidase and exo-1, 4-β-glucanase, which occur in fermentation broths and industrial enzyme preparations [6,9]. Furthermore, several methods have been reportedly used for the detection of endoglucanase hydrolases activity [10]. Among these methods, High Performance Liquid Chromatography (HPLC) and mass spectrometry methods need complicated instruments, and the colorimetric and fluorescence assay needs special derivative reagents [11–13]. Yet, the colorimetric methods including DNS and AuNP methods are competitive, but they still have several drawbacks such

E-mail address: f_fatemi@sbu.ac.ir.

https://doi.org/10.1016/j.ijbiomac.2020.01.030
0141-8130/

as the requirement of experienced professional for the sample preparation and analysis [14–16]. Considering the commercial importance of endoglucanase enzymes, development of a specific and robust detection method is an important step in any cellulose application process [17–19]. Many efforts have been devoted to the development of new generation of biosensors to circumvent these drawbacks, using nucleic acid as the biorecognition element [20–22]. Aptamers are short single-stranded DNA/RNA molecules that bind to their preselected targets and include small substances or cells or other biomolecules with high selectivity and affinity [22,23]. Ease of synthesis, thermal stability, and low cost are some features of aptamers. There is a new category of biosensors based on aptamers, called "aptasensors" [24,25]. The selectivity of aptasensors is related to their conformational changes upon binding to target molecules that provide a high selectivity for them. The union of electrochemical technique with aptamers generates the electrochemical aptasensors that act as a powerful and sensitive tool in biosensing detection [19,26]. Over recent years, introducing a wide range of nano-structure material as a transducer element strongly improved the biosensor performance and revolutionized the biosensing process [20,27]. Graphene-based nanocomposites are now popular substrates in various fields of application, due to their unique physical and chemical advantageous properties. Using graphene oxide and reduced graphene oxide (RGO) in biosensor design not only overcomes the limitations of the usage of a single component in biosensor applications, but also provides a more effective surface area, higher specificity, limit of detection (LOD) and excellent catalytic properties [28]. The oxygen functionalities on reduced graphene oxide produce an overall negative zeta potential, and easing coupling with positively charged nanomaterials. Nowadays, the gold nanoparticles (AuNPs) are considered as the most promising nanomaterial for design of a new generation of biosensors [23]. Due to their large surface area, excellent conductivity and effectively conjugation with thiolated motifs, the AuNPs have been widely used in the construction of electrochemical biosensors [22,29]. The addition of Au nanoparticles acts as a nano-spacer and conductor, thus, enhancing the graphene interlayer distance to minimize the aggregation and agglomeration. Furthermore, functionalization of RGO with AuNPs enhances the loading efficiency of the biomolecules and consequently increases the electrical conductivity of RGO [30,31].

The aim of this study is to develop a specific method for the identification and measurement of endoglucanase. There are no previous reports of sensitive and selective detection of endoglucanase through the aptamer, and thus the present research represents the first attempt to do so. Moreover, the process described here could become the basis for highly sensitive detection of various enzymes. In this work, we designed and constructed a new aptasensor electrode for detection of endoglucanase type II (EG II), which is one of the most common endoglucanases and accounts for 5–10% of the total cellulase [1]. The biosensor electrode was fabricated using RGO/AuNPs and an aptamer chain. After fabrication of the aptasensor electrode, its electrochemical response was studied using electrochemical technique.

2. Materials and methods

2.1. Chemicals and reagents

Analytical-grade reagents were used as received without any pretreatment. Double-distilled water was used for the preparation of solutions. Graphite powder, tris-hydroxymethylaminomethane hydrochloride (Tris) and $K_3[Fe(CN)_6]$, gold chloride ($HAuCl_4$), sodium borohydride ($NaBH_4$), Sulfuric acid(H_2SO_4), Potassium permanganate ($KMnO_4$) were obtained from Merck. Twenty millimolar Tris-HCl buffer (pH 7.4) containing 140 mM NaCl, 5 mM KCl, 1 mM $CaCl_2$, and 1 mM $MgCl_2$ were used as a binding buffer. Phosphate-buffered solution (PBS) (pH 7.0, 0.1 M) containing10 mM KCl and 2 mM $MgCl_2$ was used as the working buffer solution. All other chemicals were analytical grade and used as received.

The DNA aptamer was selected from an initial pool of 10^{15} different ssDNAs with 30-nt central block of randomized sequence, through the Systematic evolution of ligands by exponential enrichment (SELEX) using nitrocellulose membrane and protein blotting method on the solid support [32]. At the same time, aptamer enrichment during different SELEX phases were investigated by Real-time PCR. The affinity of selected aptamer to Endoglucanase II was calculated by fluorimetric method [33]. The selected ssDNA with 3′-SH_2 modification used in this study was custom-synthesized by the Bioneer Co. (South Korea), and the sequence of aptamer was as follows: 5′-AGACAAGGAAAATCCT TCAATGAAGTGGGTCG-SH2-3′ (EgII aptamer containing 32 bases).

The Endoglucanase II, Xylanase and Phytase were produced recombinantly in *P. pastoris* following previous reports and β-glucosidase was purchased from sigma [34–36].

2.2. Synthesis of RGO/AuNPs

RGO/AuNPs were synthesized as in previous reports [37]. At first, commercial graphite was used to synthesis the graphene oxide according to Hummers method [37,38]. Graphite (10 g) and H_2SO_4 (230 mL) were stirred at a temperature below 20 °C and then $KMnO_4$ was added to the suspension. After that, the temperature was changed to 40 °C and the mixture was stirred for 1 h. At this time, 500 mL of deionized water was added to the mixture and the temperature was increased to 100 °C. H_2O_2 was then added, followed by addition of deionized water, until the filtrate became neutral and the remaining impurities were removed. The suspension was then washed with HCl and deionized water. After that, the product was exfoliated in deionized water and 5 g of $NaBH_4$ was added to form graphene oxide (GO) nanosheets; the product was then incubated at 100 °C for 24 h. RGO/AuNPs were synthesized by adding 0.25 M $HAuCl_4{\cdot}6H_2O$ to the GO nanosheets and sonicated for 10 min, followed by 3 h of incubation at 40 °C. The final product was filtered using a Buchner funnel, washed with deionized water three times, and then dried at 50 °C for 12 h.

2.3. RGO/AuNP characterizations

Morphological investigations were carried out by using a Transmission Electron Microscopy TEM (Zeiss - EM10C - 100 KV) and energy-dispersive X-ray spectroscopy (EDX). The X-ray diffractometer (PANalytical X'Pert-Pro) had a Cu-Kα monochromatized radiation source and a Ni filter. X-ray was used to obtain the diffraction patterns of RGO/AuNPs.

2.4. Fabrication of aptasensor electrode

The glassy carbon electrode (GCE) was polished with 0.03 M alumina slurry and washed with large amount of distilled water. Then RGO/AuNP/aptamer/Nafion-modified GCE was then fabricated by placing some of RGO/AuNP/aptamer/Nafion dropped on the electrode surface to form a homogeneous layer.

RGO/AuNP/aptamer/Nafion was prepared as follows: 2 mg/mL RGO/AuNPs was incubated with 2 μM thiolated EGII aptamer for 24 h at 4 °C. The RGO/AuNP/aptamer was then incubated with 0.1% *w*/w Nafion at a 1:4 ratio for 10 min at ambient temperature. 5 μM of RGO/AuNP/aptamer/Nafion was dropped to the electrode surface and dried at ambient condition and inert atmosphere. Afterwards, the fabricated electrode was rinsed with water to eliminate any unbounded aptamers and finally incubated with different concentrations of EGII for 45 min. The designed aptasensor was stored at 4 °C when not in use. The electrochemical signal was measured in a solution containing 1 mM $K_3[Fe(CN)_6]$ by using CV.

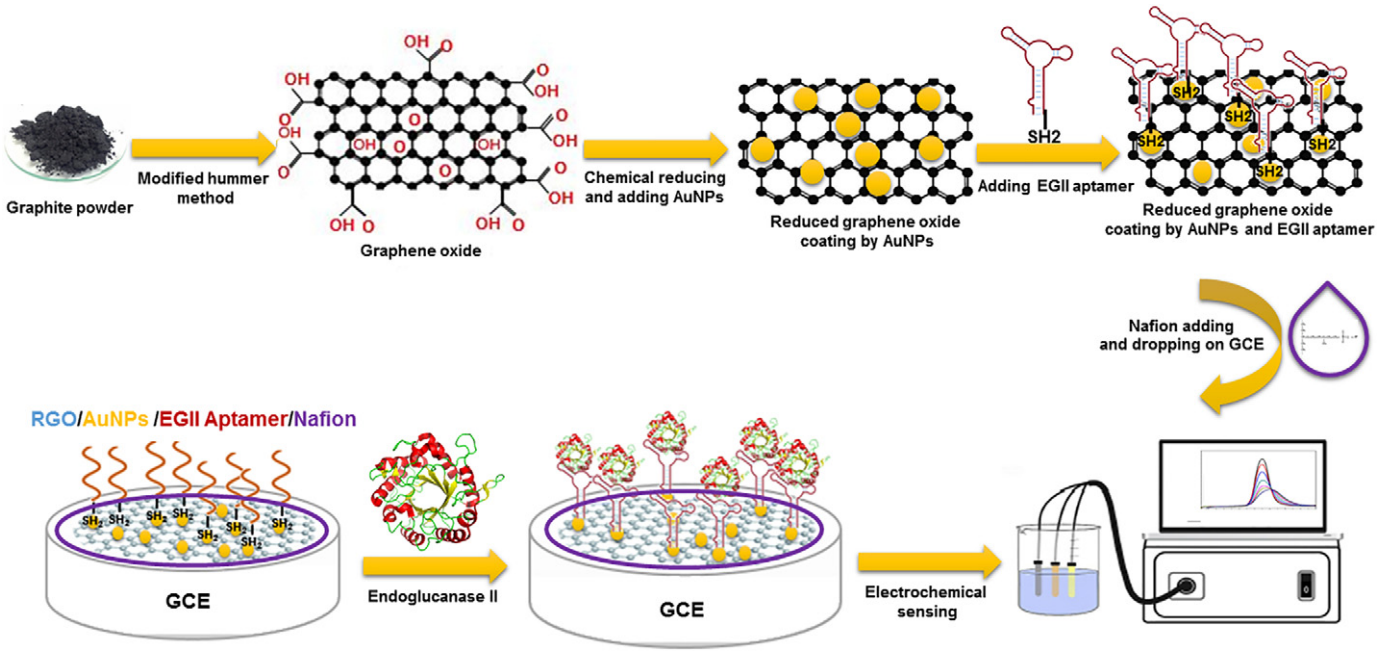

Scheme 1. Principle of endoglucanase aptasensor. The graphene oxide and reduced graphene oxide synthesized. Then the reduced graphene oxide (RGO)/Au nanoparticles/EGII aptamer/Nafion modified glassy carbon electrode (GCE) was fabricated by placing some of RGO/AuNPs/EGII aptamer/Nafion dropped on the electrode surface. 5′-thiolated EGII-DNA aptamer self-assemble and binds to the AuNPs. The Endoglucanase binds to the immobilized aptamer, forming a complex. Square wave voltammetry (SWV) technic measure the difference in faradic current in the presence of different concentration of Endoglucanase.

2.5. Electrochemical measurements

All electrochemical experiments were performed by an Autolab General Purpose System PGSTAT 30 (Eco-chime, Netherlands). The electrochemical experiments were conducted using a conventional three-electrode cell with an Ag/AgCl reference electrode (Argental, 3 M KCl). For the counter electrode, a platinum wire with a diameter of 0.5 mm and an exposed area of 0.65 cm^2 was used. A glassy carbon electrode with an area of 0.03 cm^2 was used as the working electrode.

CVs of the fabricated electrode were performed in 5 mM $K_3[Fe(CN)_6]$ solution containing 0.2 M KCl, scanning from −0.6 to 0.7 V at a scan rate of 50 mV s^{-1}. Squarewave voltammetry (SWV) was performed in 0.1 M PBS (pH 7.0) to evaluate the performance and time processing of the aptasensor. The SWV measurement was carried out: the potential range was from −0.6 to 1.1 V, modulation amplitude was 0.05 V, pulse width was 0.05 s, and sample width was 0.0167 s.

Limit of detection (LOD) and limit of quantification were calculated by the following equations:

$$LOD = 3sb/m \quad (1)$$

$$LOQ = 10sb/m \quad (2)$$

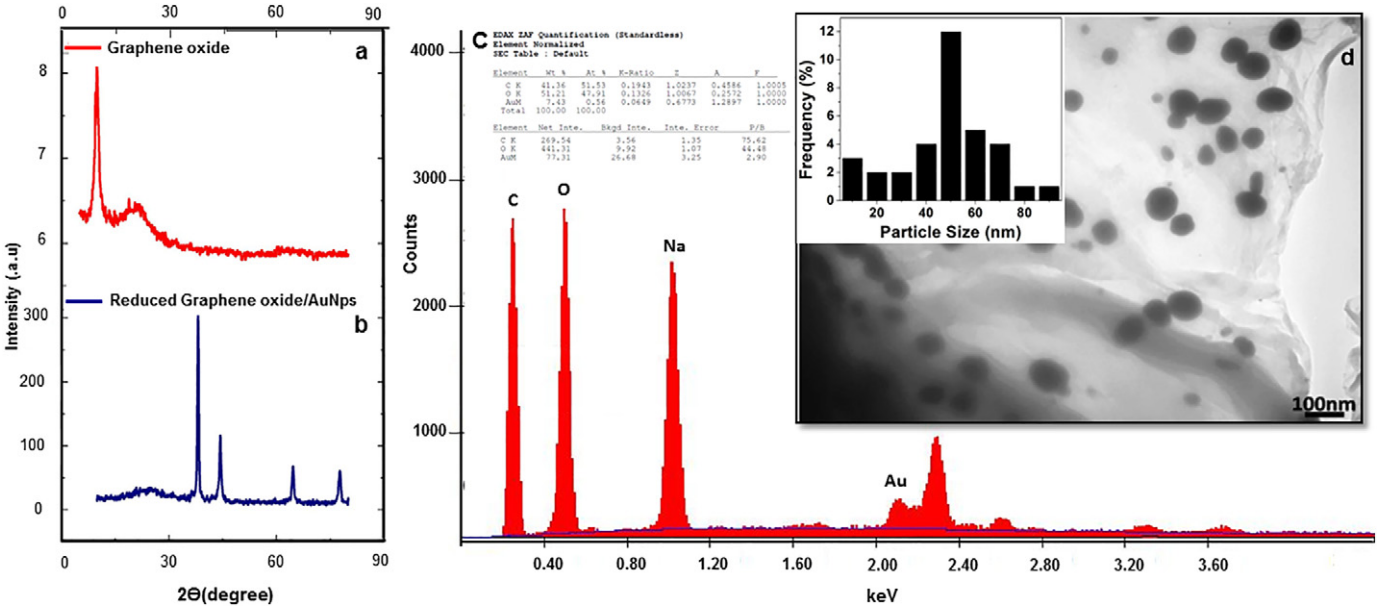

Fig. 1. (a) XRD analysis of GO powder and (b) RGO/AuNPs. (c) EDX analysis (d) TEM image of RGO/AuNPs and histogram of particle size distribution.

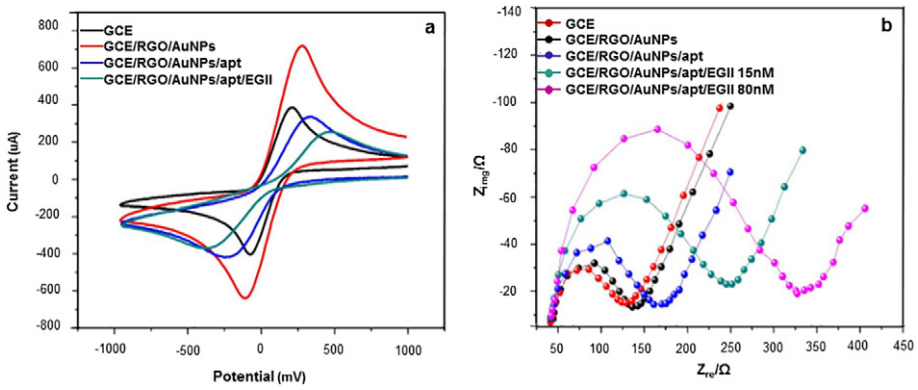

Fig. 2. (a) CVs of modified electrodes with RGO/AuNPs, RGO/AuNPs/Apt and RGO/AuNPs/Apt/EGII in 1 mM $K_3[Fe(CN)_6]$ solution at the scan rate of 50 mV s^{-1} and (b) EIS spectra modified electrode with RGO/AuNPs, RGO/AuNPs/Apt and RGO/Au NPs/Apt/EGII 15 nM and 80 nM.

where Sb is the standard deviation of blank solution and m is the slope of calibration curve. LOD of EGII was calculated about 0.1 nM and the value of LOQ was determined about 0.33 nM.

2.6. Real sample preparation

The slurry sugarcane bagasse sample was prepared following the protocol reported by H. Jørgensen [39]. 50 mL biomass samples were spiked with appropriate concentration of endoglucanase enzyme. The mixture was then centrifuge at 10,000 ×*g* for 15 min. The supernatant was filtered using 0.45 μm syringe filter and store at 4 °C for further analysis.

3. Results and discussion

3.1. RGO/AuNPs nanoparticles surface characterization

We designed an aptasensor platform using the principle described in (Scheme.1). The surface morphology and characterization of GO and RGO/AuNPs powder were investigated by TEM, XRD and EDX. Fig. 1a presents the XRD diagram of GO powder and RGO/AuNPs. As shown, a strong and sharp peak at $2\theta = 11.2°$ demonstrated formation of GO. The small peak observed at $2\theta = 24.2°$ is associated with the (100) plane of graphite and indicates that small amounts of graphite phases are still present in the GO. As illustrated in Fig. 1b, the XRD diagram of RGO/Au NPs presents the broad peak at around $2\theta = 24°$ and can be indexed into the RGO sheets. Furthermore, the diffraction peaks at 38.1, 64.5, and 77.5° correspond to (111), (220), and (311) planes of AuNPs, respectively. Moreover, an additional peak is observed at about 43.6°, which seems to be due to overlapping (200) reflection plane of Au, at $2\theta = 44.4°$, with (100) plane of graphite. The results of EDX and TEM are present in Fig. 1c and d. EDX analysis confirmed that the weight percentage of AuNPs is low and the nanoparticles are very small in size. As evident from Fig. 1d, the RGO sheets exhibit rippled and crumpled morphology and have a structure consisting of very thin layers. The TEM images of AuNPs/RGO sheets indicate a uniform and homogeneous distribution for gold nanoparticles at the surface of RGO sheets with the surface coverage of about 5.6%. Also, an average particle size of 50 nm, from the size distribution histogram (inset) could be estimated. To obtain the size distribution histograms, about 100 nanoparticles were considered for each sample.

3.2. Characterization of electrochemical behavior of fabricated aptasensor

The aptasensor electrochemical behavior was characterized in presence of a redox probe and by using the Cyclic Voltammetry (CV) and Electrochemical Impedance Spectroscopy (EIS) technique. The Fig. 2a presents the CVs of electrodes through aptasensor fabrication process in 1 mM $K_3[Fe(CN)_6]$ solution with a scan rate of 50 mV s^{-1}. As illustrated, a well-defined redox peak of $[Fe(CN)_6]^{3-/4-}$ was observed at the bare GCE (black line). The red line curve shows the CV of the RGO/AuNP modified electrode (GCE/RGO/AuNPs). The peak current was markedly increased, indicating that the RGO/AuNPs load on the electron surface area, change the electron transfer resistance and therefore promote electron transfer. After that, the thiolated aptamer chains were self-assembled at the surface of (GCE/RGO/AuNPs) and the peak current clearly decreased. The result illustrates that the RGO/AuNPs are well decorated by EGII aptamer chains.

The current response of $[Fe(CN)_6]^{3-/4-}$ on the GCE/RGO/AuNP/apt/EGII (green line) was further decreased, indicating that the EGII successfully interacts with aptamer chains. The pattern shows that the modified electrode can strongly detect this protein.

The Nyquist diagrams of the electrode modification procedure are presented in Fig. 2b. As can be seen, each diagram has a semi-circle

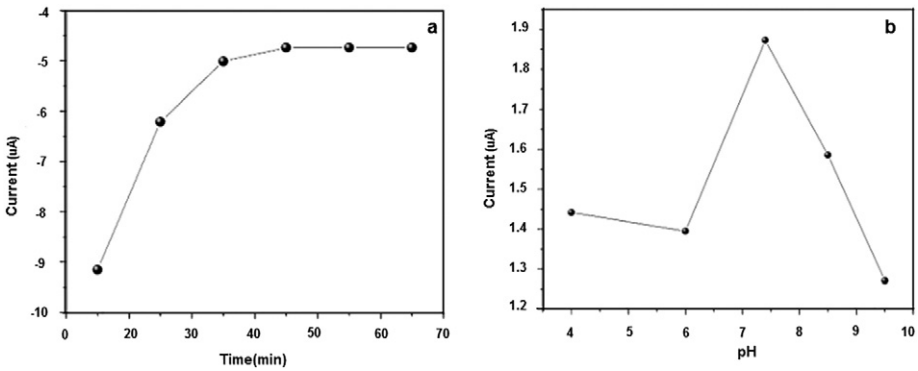

Fig. 3. (a) Time processing EGII aptasensor and the effect of time incubation upon SWV. (b) The effect of pH on the response of aptasensor.

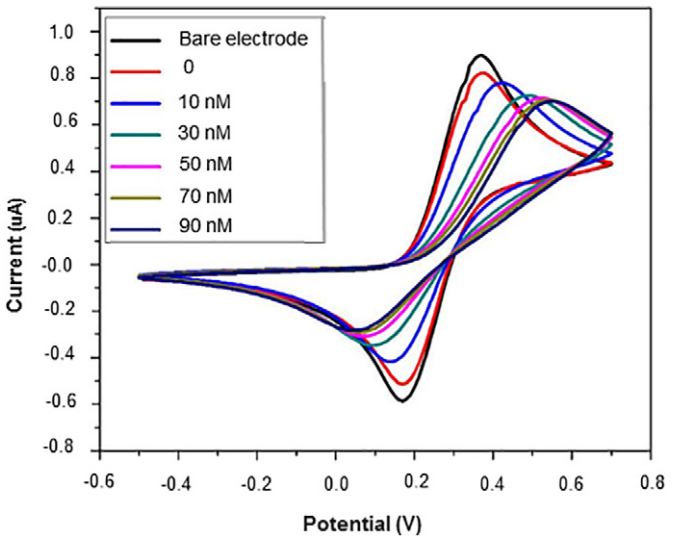

Fig. 4. CVs of RGO/AuNPs/Apt modified electrodes in presence of various concentration of EGII at the scan rate of 50 mV s^{-1}, in 1 mM $K_3[Fe(CN)_6]$ solution.

that corresponds to charge transfer resistance of the Fe^{2+}/Fe^{3+} reaction. The values of electron transfer resistance (R_{ct}) of 90 Ω are measured for the GCE bare electrode while the modified electrodes show a higher R_{ct} value respectively; 105 Ω for GCE/RGO/AuNPs modified electrode, 160 Ω for GCE/RGO/AuNP/apt modified electrode, 260 Ω and 325 Ω for GCE/RGO/AuNP/apt/EGII modified electrode respectively, in presence of different concentration of endoglucanase II. As reveled by the R_{ct} value, by attaching the aptamer chains on the surface of RGO sheets, the electrochemical conductivity of the modified electrode decreased, which resulted in increasing the charge transfer resistance of the electrochemical reaction. Indeed aptamer/enzyme complex interaction caused occupation of available active sites on the electrode surface and increased the resistance, resulting in increased Nyquist diameter.

3.3. Physiochemical conditions and incubation time optimization

A number of optimizations to develop an efficient aptasensor for sensitive detection of endoglucanase have been performed. The time processing and the effect of time incubation between aptamer and the EGII enzyme were analyzed by SWV. As shown in Fig. 3a, the differential pulse voltammetric response increased by increasing incubation time. The signal values stabilized after 35 min and remained stable for the rest of the measurement of the time. Consequently, the constant value obtained after 35 min showed that the surface of fabricated aptasensor saturated by EGII enzyme and no improvement in response could be achieved by longer incubation time.

The effect of physicochemical conditions including ionic concentration and pH was also studied. In our study, increased concentration of NaCl resulted in little decrease of endoglucanase detection, which indicated that ionic strength weakly influenced the affinity of the endoglucanase aptamer used in this study (data not shown). To investigate the influence of pH, the response of aptasensor tested in different pH ranges (Fig. 3b). The binding of the Endoglucanase to the aptamer depends on pH condition, which is probably connected to stabilizing the three dimensional aptamer conformation, optimal for binding the enzyme. Our results show that maximal response of the endoglucanase sensor occurred for pH 7.2, while for lower and higher pH the sensitivity was lower. Consequently, to ensure the aptasensor to operate at its maximum sensitivity, all the endoglucanase sensing experiments carried out in PBS at pH 7.2. The effect on temperature change wasn't investigated in our experiments and tests were performed in ambient temperature.

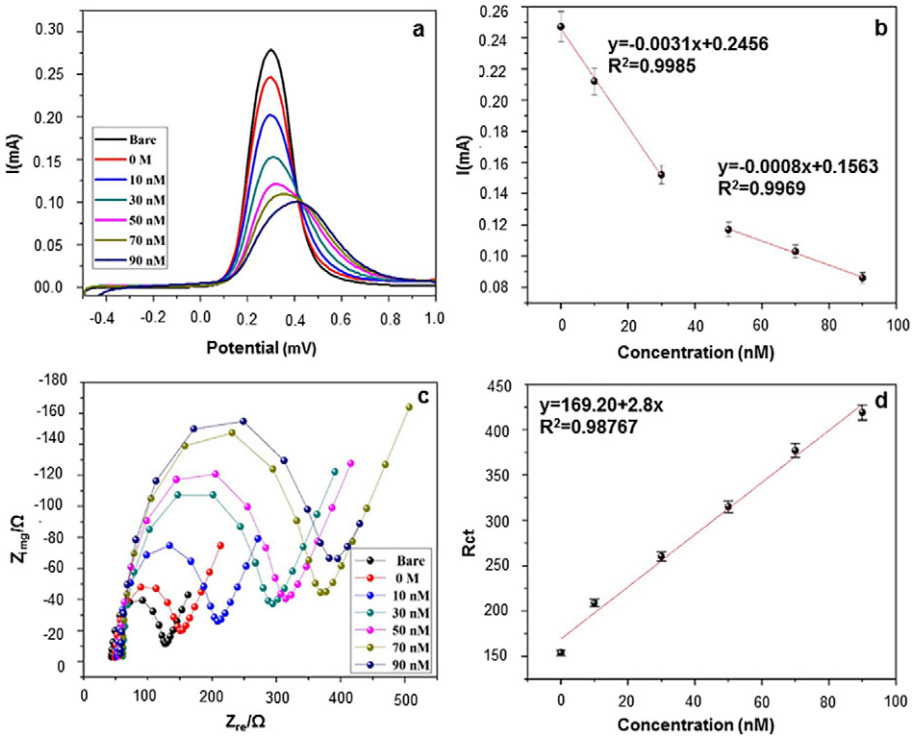

Fig. 5. (a) SWV response of electrochemical aptasensor for EGII at different concentration: 0 nm, 10 nM, 30 nM, 50 nM, 70 nM and 90 nM in detection buffer containing 0.05 M PBS (b) the calibration plot of current intensity vs concentration (nM) in the range from 0 nM to 90 nM. (c) EIS spectra for modification of aptasensor electrode at different concentration: 0 nm, 10 nM, 30 nM, 50 nM, 70 nM and 90 nM. (d) The calibration plot of modified electrode obtained from EIS spectra.

Table 1
Comparison of the analytical performance of developed EGII biosensors with other endoglucanase detection methods.

Detection method	Main examine reagent	Activity/detection limit (as reported)	Analyze time	Reference
CMC	Carboxy methyl cellulose	Not reported	>2 h	[7]
BzCNPG3	BzCNPG3 (4,6-O-benzylidene end-blocked 2-chloro-4-nitrophenyl-b-cellotrioside)	10^{-3} U	>30 min	[5]
Chito based assay	Chito-oligosaccharides	6 mU	>1 h	[14]
Flow cytometry	3-carboxy-7-(4′-aminophenoxy) coumarin, vanadium bromoperoxidase	Range of 0.1 to 0.5 U/mL	>30 min	[12]
Mass spectroscopy	ABTS mediator (2,2′-azino-bis(3-ethylbenzothiazoline-6-sulfonic acid))	–	>2 h	[11]
HPLC based FPA assay	3, 5-dinitrosalicylic acid	63.7 ± 1.5 FPU/mL	>1 h	[10]
AuNPs	CTAC, hydrogen tetrachloroaurate hydrate	0.14 IU mL^{-1}	>45 min	[13]
Endoglucanase aptasensor	GCE/RGO/AuNPs/apt	0.1 nM	~30 min	This work

3.4. Analytical performance characteristics of EGII aptasensor

The electrochemical performance of designed aptasensor is investigated in various concentration of EGII enzyme in $K_3[Fe(CN)_6]$ solution. As illustrated in Fig. 4, each CV curve has a redox peak related to electrochemical reaction of Fe^{2+}/Fe^{3+}. Following interaction between aptamer and enzyme, available active site on the electrode surface decreased and the steric hindrance on the electrode surface area increased. Therefore, the magnitude of the redox peak current diminished. Consequently, the interaction procedure caused an increase in the electrode surface resistance, resulting in a reduction in the anodic and cathodic peaks and a change in the peak potential to positive for oxidation and negative for reduction processes. As the single-stranded DNA aptamer molecules contain numerous negatively charged phosphate groups, they are likely to act as a barrier to restricting access of the anionic electrolyte to the electrode surface [24]. By enhancing the concentration of EGII at the surface of electrode, the anodic peak potential shifted from 0.3 to 0.6 V and the cathodic changed from 0.2 to 0 V. This accounted for the increase in Ret for the aptamer/AuNPs coated electrode. The larger semicircle indicative of further enhance in Ret occurred from formation of a mixed layer comprising aptamer and enzyme molecules.

SWV is one of most useful electrochemical techniques for analytic quantitation. Because of the elimination of double-layer charge for high-surface-area electrodes, the sensitivity of this technique is very useful for detection of analytes in very low concentrations. Square wave curves of RGO/AuNP/apt at various concentration of EGII are presented in Fig. 5a. As shown, by increasing the concentration of EGII and therefore occupation of active sites at the surface of electrode, the magnitude of the peak current decreased. The calibration curve of modified electrode is shown in Fig. 5b. We can see the dual behavior of the modified electrode at linear range concentrations of EGII. By changing the concentration of EGII, the slope of the calibration curve shifted from higher magnitude at low concentration to lower magnitude at higher concentrations. This behavior corresponds to a change in binding mechanism. It is likely that the high sensitivity can be attributable to the correct orientation of the enzyme, whereas the reduced linear working range can be defined by the number of recognition sites present on the electrode surface.

Nyquist diagrams of the modified electrode at linear range from 0 to 90 nM concentrations of EGII are shown in Fig. 5c. As shown, by increasing the concentration of EGII macromolecules at the surface of electrode, the charge transfer resistance of the Fe^{2+}/Fe^{3+} electrochemical reaction increased, corresponding to semi-circle diameters. The calibration curve of EIS analysis shown in Fig. 5d and presents a linear response of the modified electrode to EGII concentration, demonstrating a satisfactory electrochemical behavior of EGII aptasensor with a limit of detection (LOD) 0.1 nM and a limit of quantitation (LOQ) value about 0.33 nM.

Comparison of the purposed aptasensor based on the GCE/RGO/AuNP/apt in this work to the other previously reported detection method for endoglucanase was presented in Table 1. The developed aptasensor achieved a wide linear dynamic range from 10 to 90 nM with a low LOD value of 0.1 nM in 30 min analysis time, which demonstrates suitable and significant performance compared to other reports.

3.5. Selectivity and sensitivity of EGII aptasensor

One of the key factors for evaluating the performance of biosensor is the selectivity. To investigate the selectivity of EGII aptasensor, the SWV response to some other enzymes such as xylanase, phytase and β-glucosidase at concentration of 50 nM were analyzed under the same experimental conditions. As illustrated in Fig. 6, the biosensor showed a specific response to EGII which was at least ten times higher than that of xylanase, phytase and β-glucosidase. The sensitivity of purposed aptasensor was investigated from the slope of the linear part of the calibration curve (Fig. 5, curve d). In the electrochemical measurements, the sensitivity was 2.8 nM. These results show that the EGII aptasensor has the higher sensitivity and selectivity toward the endoglucanase II than the other enzymes.

3.6. Stability and reproducibility of EGII aptasensor

The stability of the aptasensor was investigated at 30 day period and it was evaluated every two weeks for long-term storage at 4 °C. The

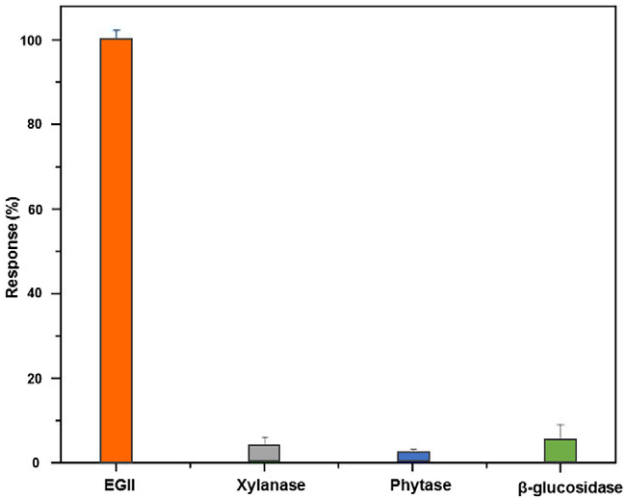

Fig. 6. RGO/AuNP/apt/aptasensor selectivity toward EGII, xylanase, phytase, β-glucosidase.

Table 2
Recoveries of endoglucanase from spiked biomass samples ($n = 3$).

Samples	Added (nM)	Found (nM)	Recovery (%)	RSD (%)
1	0	0	–	1.7
2	0.05	0.048	89%	3.2
3	5	4.94	94%	3.4
4	50	50.66	112.5%	5.3

aptasensor maintained 96% of its initial current response after 15 days storage and 92% after 30 days of storage, which demonstrated that the aptasensor has a good stability. To evaluate the reproducibility of EGII aptasensor, five proposed aptasensors were fabricated under the same condition and incubated in presence of 40 nM enzyme. The electrochemical response by independently prepared aptasensors was similar with the relative standard deviation (RSD) of 3.5%. This result demonstrated acceptable precision and reproducibility of proposed aptasensor.

3.7. Real sample analysis

To evaluate the practicability and reliability of prepared aptasensor for analysis in real sample, the recovery experiments for several samples were assayed. The biomass samples were spiked with various concentration of endoglucanase enzyme in the range of (5×10^{-8} -5×10^{-2}). Sugarcane bagasse biomass samples containing endoglucanase was diluted 1:10 in PBS buffer. The EIS spectra were carried out after incubation of the aptasensor for 35 min at ambient temperature with the samples. As shown in Table 2, the recovery values range from 89% to 112.5% and relative standard deviation from 3.2% to 5.3% for sugarcane bagasse biomass. The results indicated that the purposed aptasensor could be applied for the detection of endoglucanase in biological sample.

4. Conclusions

Given the importance of endoglucanase as an industrial biocatalyst in a wide range of industries, there is an increasing global demand for a rapid, specific, automatable assay that exhibits a desirable recovery in the determination of endoglucanase levels. In the present study, we report for the first time the sensitive and selective detection of endoglucanase through aptamer. The electrochemical sensing of endoglucanase II was studied using RGO/AuNPs/aptamer platform. Decoration of reduced graphene oxide sheets with AuNPs enabled efficient immobilization of thiolated aptamer on the surface of the electrode and enhanced the conductivity and surface area of the electrode. The designed modified electrode presents a great potential to rapid detection of endoglucanase II with suitable sensitivity and selectivity. In addition to its remarkable long-term stability and reproducibility, the purposed aptasensor showed a low limit of detection (<0.1 nM) values for endoglucanase detection. The fabricated aptasensor was successfully applied for the endoglucanase detection in real sample. Compared with the previously reported methods, the purposed aptasensor in this study has many advantages, such as ease of synthesis, simplicity of operation, low cost and specificity, and the short processing time. Furthermore, the aptasensor presented in this work can be developed for high-throughput detection, which will be more feasible for industrial application.

Author statement

Fataneh Fatemi: Investigation, Conceptualization, Methodology, Data curation, Writing- Reviewing and Editing.

Declaration of competing interest

The authors declare that they have no conflict of interest.

Acknowledgments

This work was supported by the Shahid Beheshti University G.C., research grant No. 600/53.

Ethical approval

This article does not contain any studies with human or animal subjects.

References

[1] M.A. Reeta, R. Singhania, A. Pandey, A.K. Patel, Cellulases, Current Development in Biotechnology and Bioengineering, 2017.
[2] V. Beniwal, A. Sharma, Industrial Enzymes: Trends, Scope and Relevance, 2014.
[3] D. Fapyane, E.E. Ferapontova, Electrochemical assay for a total cellulase activity with improved sensitivity, Anal. Chem. 89 (7) (2017) 3959–3965.
[4] M. Dashtban, M. Maki, K.T. Leung, C. Mao, W. Qin, Cellulase activities in biomass conversion: measurement methods and comparison, Crit. Rev. Biotechnol. 30 (4) (2010) 302–309.
[5] B.V. McCleary, D. Mangan, R. Daly, S. Fort, R. Ivory, N. McCormack, Novel substrates for the measurement of endo-1,4-beta-glucanase (endo-cellulase), Carbohydr. Res. 385 (2014) 9–17.
[6] D. Mangan, C. Cornaggia, V. McKie, T. Kargelis, B.V. McCleary, A novel automatable enzyme-coupled colorimetric assay for endo-1,4-beta-glucanase (cellulase), Anal. Bioanal. Chem. 408 (15) (2016) 4159–4168.
[7] H.R. Johnsen, K. Krause, Cellulase activity screening using pure carboxymethylcellulose: application to soluble cellulolytic samples and to plant tissue prints, Int. J. Mol. Sci. 15 (1) (2014) 830–838.
[8] Z. Altintas, M.J. Abdin, A.M. Tothill, K. Karim, I.E. Tothill, Ultrasensitive detection of endotoxins using computationally designed nanoMIPs, Anal. Chim. Acta 935 (2016) 239–248.
[9] Y. Wang, Q. Hu, T. Tian, Y. Gao, L. Yu, A liquid crystal-based sensor for the simple and sensitive detection of cellulase and cysteine, Colloids Surf. B: Biointerfaces 147 (2016) 100–105.
[10] Y.H. Percival Zhang, M.E. Himmel, J.R. Mielenz, Outlook for cellulase improvement: screening and selection strategies, Biotechnol. Adv. 24 (5) (2006) 452–481.
[11] D. Chu, H. Deng, X. Zhang, J. Zhang, J. Bao, A simplified filter paper assay method of cellulase enzymes based on HPLC analysis, Appl. Biochem. Biotechnol. 167 (1) (2012) 190–196.
[12] R.E. Goacher, E.A. Edwards, A.F. Yakunin, C.A. Mims, E.R. Master, Application of time-of-flight-secondary ion mass spectrometry for the detection of enzyme activity on solid wood substrates, Anal. Chem. 84 (10) (2012) 4443–4451.
[13] R. Ostafe, R. Prodanovic, U. Commandeur, R. Fischer, Flow cytometry-based ultra-high-throughput screening assay for cellulase activity, Anal. Biochem. 435 (1) (2013) 93–98.
[14] L. Shen, C. Wang, J. Chen, Photometric determination of the activity of cellulase and xylanase via measurement of formation of gold nanoparticles, Microchim. Acta 184 (1) (2016) 163–168.
[15] A.R. Ferrari, Y. Gaber, M.W. Fraaije, A fast, sensitive and easy colorimetric assay for chitinase and cellulase activity detection, Biotechnol. Biofuels 7 (1) (2014) 37.
[16] K.K. Kwon, S.J. Yeom, D.H. Lee, K.J. Jeong, S.G. Lee, Development of a novel cellulase biosensor that detects crystalline cellulose hydrolysis using a transcriptional regulator, Biochem. Biophys. Res. Commun. 495 (1) (2018) 1328–1334.
[17] Z. Altintas, M. Gittens, J. Pocock, I.E. Tothill, Biosensors for waterborne viruses: detection and removal, Biochimie 115 (2015) 144–154.
[18] K. Sefah, J.A. Phillips, X. Xiong, L. Meng, D. Van Simaeys, H. Chen, J. Martin, W. Tan, Nucleic acid aptamers for biosensors and bio-analytical applications, Analyst 134 (9) (2009) 1765–1775.
[19] B. Piro, S. Shi, S. Reisberg, V. Noel, G. Anquetin, Comparison of electrochemical immunosensors and aptasensors for detection of small organic molecules in environment, food safety, clinical and public security, Biosensors (Basel) 6 (1) (2016).
[20] H. Jo, C. Ban, Aptamer-nanoparticle complexes as powerful diagnostic and therapeutic tools, Exp. Mol. Med. 48 (2016) e230.
[21] S. Ranjbar, S. Shahrokhian, Design and fabrication of an electrochemical aptasensor using Au nanoparticles/carbon nanoparticles/cellulose nanofibers nanocomposite for rapid and sensitive detection of Staphylococcus aureus, Bioelectrochemistry 123 (2018) 70–76.
[22] P. Szustakiewicz, N. Kolsut, A. Leniart, W. Lewandowski, Universal method for producing reduced graphene oxide/gold nanoparticles composites with controlled density of grafting and long-term stability, Nanomaterials (Basel) 9 (4) (2019).
[23] K.M. Song, S. Lee, C. Ban, Aptamers and their biological applications, Sensors (Basel) 12 (1) (2012) 612–631.
[24] Q. Wang, X. Qin, L. Geng, Y. Wang, Label-free electrochemical aptasensor for sensitive detection of malachite green based on Au nanoparticle/graphene quantum dots/tungsten disulfide nanocomposites, Nanomaterials (Basel) 9 (2) (2019).
[25] Y. Li, R. Wang, Aptasensors for detection of avian influenza virus H5N1, Methods Mol. Biol. 1572 (2017) 379–402.
[26] C.V. Ocaña, M, Impedimetric Aptasensors Using Nanomaterials, Nanotechnology and Biosensors Advanced Nanomaterials, Elsevier, 2018 233–267.
[27] C. Zhang, C. Lai, G. Zeng, D. Huang, L. Tang, C. Yang, Y. Zhou, L. Qin, M. Cheng, Nanoporous Au-based chronocoulometric aptasensor for amplified detection of Pb

(2+) using DNAzyme modified with Au nanoparticles, Biosens. Bioelectron. 81 (2016) 61–67.
[28] D. He, C. Zhang, G. Zeng, Y. Yang, D. Huang, L. Wang, H. Wang, A multifunctional platform by controlling of carbon nitride in the core-shell structure: from design to construction, and catalysis applications, Appl. Catal. B Environ. 258 (2019).
[29] L. Qin, H. Yi, G. Zeng, C. Lai, D. Huang, P. Xu, Y. Fu, J. He, B. Li, C. Zhang, M. Cheng, H. Wang, X. Liu, Hierarchical porous carbon material restricted au catalyst for highly catalytic reduction of nitroaromatics, J. Hazard. Mater. 380 (2019), 120864.
[30] I. Khalil, N.M. Julkapli, W.A. Yehye, W.J. Basirun, S.K. Bhargava, Graphene-gold nanoparticles hybrid-synthesis, functionalization, and application in a electrochemical and surface-enhanced Raman scattering biosensor, Materials (Basel) 9 (6) (2016).
[31] L. Qin, G. Zeng, C. Lai, D. Huang, C. Zhang, P. Xu, T. Hu, X. Liu, M. Cheng, Y.P. Liu, L. Hu, Y. Zhou, A visual application of gold nanoparticles: simple, reliable and sensitive detection of kanamycin based on hydrogen-bonding recognition, Sensors Actuators B Chem. 243 (2017) 946–954.
[32] L. Qiao, B. Lv, X. Feng, C. Li, A new application of aptamer: one-step purification and immobilization of enzyme from cell lysates for biocatalysis, J. Biotechnol. 203 (2015) 68–76.
[33] M. pouryaghubi, H. Kouchakzadeh, S.O. Ranaei Siadat, Efficient purification of recombinant Endo-ß-glucanase II directly from culture broth utilizing aptamer-modified magnetic nanoparticles, Iran. J. Biotechnol. (in (press)).
[34] A. Akbarzadeh, S.O. Ranaei Siadat, M. Motallebi, M.R. Zamani, M. Barshan Tashnizi, S. Moshtaghi, Characterization and high level expression of acidic endoglucanase in Pichia pastoris, Appl. Biochem. Biotechnol. 172 (4) (2014) 2253–2265.
[35] A. Akbarzadeh, S.O. Ranaei Siadat, M.R. Zamani, M. Motallebi, M. Barshan Tashnizi, Comparison of biochemical properties of recombinantendoglucanase II of Trichoderma reesei in methylotrophic yeasts, Pichia pastoris and Hansenula polymorpha, Proc. Biol. Sci. 3 (2013) 108–117.
[36] B.O. Kaur, H. S, B.S. Chadha, Comparative analysis of two catalytically distinct endoglucanases from Aspergillus nidulans, J. Appl. Biomater. Biomech. 3 (2) (2015) 22–29.
[37] J. Shabani Shayeh, A. Ehsani, M.R. Ganjali, P. Norouzi, B. Jaleh, Conductive polymer/reduced graphene oxide/Au nano particles as efficient composite materials in electrochemical supercapacitors, Appl. Surf. Sci. 353 (2015) 594–599.
[38] M. Pourmadadi, J.S. Shayeh, M. Omidi, F. Yazdian, M. Alebouyeh, L. Tayebi, A glassy carbon electrode modified with reduced graphene oxide and gold nanoparticles for electrochemical aptasensing of lipopolysaccharides from Escherichia coli bacteria, Mikrochim. Acta 186 (12) (2019) 787.
[39] H. Jorgensen, Test of efficacy of cellulases for biomass degradation, Methods Mol. Biol. 1796 (2018) 283–297.